Experiment 7: Diffraction and Interference

Naim Ayat

30 November 2017

Thursday 11:00AM PST

David Bauer

Lab Partner: Adam Jankowski

7.4.1 Worksheet

1. We observe that as the double slit spacing increases, the diffraction peaks become closer together.
2. Single slit interference is responsible for the shape of the intensity curve's envelope. Meanwhile, double slit interference is responsible for oscillations within the envelope.

7.4.2 Presentation Report

2. Introduction

This experiment serves to examine the wave-like nature of light while investigating the properties of single, double, and multiple slit diffraction and interference. From a lab configuration including a laser, photometer, and slits to induce diffraction, we will generate data plots relating intensity to distance for various diffraction scenarios. We note that a single slit diffracting element follows the model:

$$b\sin(\theta) = \lambda m \tag{1}$$

where b is the width of the slit, θ is the angle of light from the slit to the screen, and λ is the light's wavelength. Also, where x is the distance from the center of the diffraction pattern to a minimum on the wave and D is the distance of the diffracting element to the photometer, the approximation $\sin(\theta) \approx \tan(\theta)$ holds where $\tan(\theta) = \frac{x}{D}$. Thus, we can rewrite equation (1) as:

$$b = \frac{\lambda m D}{x}. \tag{2}$$

Using our intensity vs. distance data, we will solve for b in equation (2). We will then compare our experimental value for b to the actual slit width, verifying that our data corroborates equation (1).

Similarly, double slit diffraction follows the model:

$$d\sin(\theta) = \lambda m. \tag{3}$$

where d is the distance between slits. Once more, the approximation $\sin(\theta) \approx \tan(\theta)$ where $\tan(\theta) = \frac{x}{D}$ allows us to rewrite equation (3) as:

$$d = \frac{\lambda m D}{x}. \tag{4}$$

Again, using our intensity vs. distance data, we will calculate an experimental value for d and compare it to the actual value, verifying that our data follows equation (3).

We will also examine diffraction gratings by shining a laser through a beam expander and measuring the angles of diffraction. Using the grating equation,

$$d \sin(\theta) = \lambda n, \tag{5}$$

we will solve for the distance between gratings d and compare it to the expected value, confirming that our results agree with equation (5). Finally, we will determine the thickness of a human hair by shining a laser at it and measuring the resulting angles of diffraction.

3. Experimental Results

We attach a laser of wavelength $\lambda = 670\ nm$ to one end of a magnetic track. A potentiometer and photodiode sensor are placed on the other end. We connect the potentiometer and photodiode to a myDAQ system so that we can obtain distance and intensity measurements. The photodiode sits in the center of a translation box at the point $x = 2.5\ cm$ on the magnetic track. We align the interference patterns such that their centers occur at the same point.

A single slit slide (with a known width of $0.00004\ m$) is positioned $(0.3190 \pm 0.0005)\ m$ away from the photodiode and propagate the laser through it. We position the photodiode at $x = 1\ cm$ on the magnetic track and rotate the knob at a rate of approximately $3\frac{s}{turn}$, continuously recording data on the myDAQ system until the photodiode reaches the point $x = 4\ cm$. The resulting intensity vs. distance graph is shown in Fig. (1).

We repeat the entire procedure twice more: once for a double slit diffraction element (with a known width of $0.00004\ m$ and slit distance of $0.0000125\ m$) and once for a double slit diffraction element with unknown parameters. The resulting intensity vs. distance plots are shown in Fig. (2) and Fig. (3), respectively.

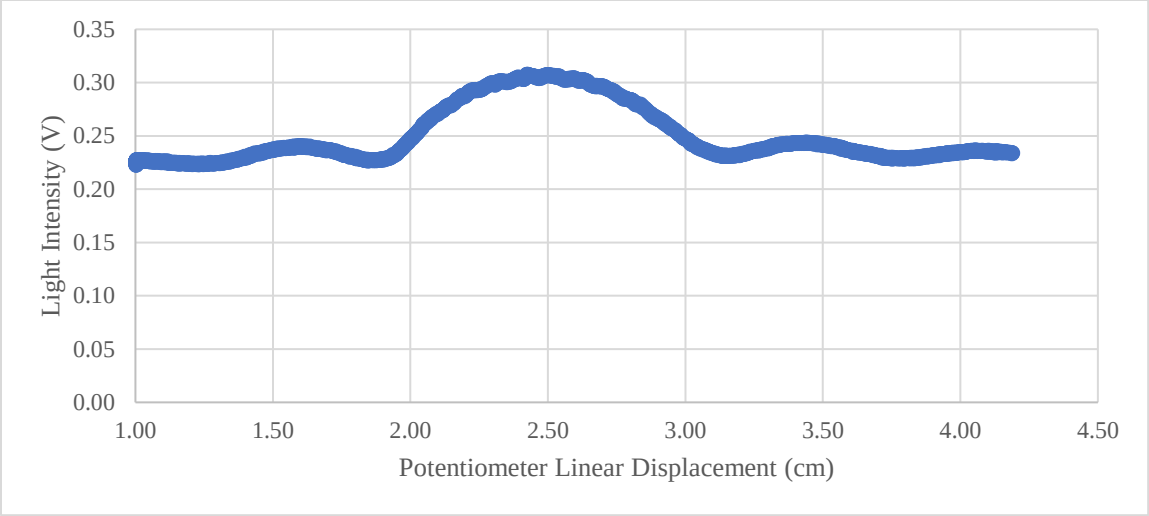

Figure 1: Diffraction Model Produced by a $0.00004\ m$-Wide Single Slit. Light intensity data is measured by the photodiode and plotted against the sensor's linear displacement along the magnetic track. The global maximum occurs at the center of the diffraction pattern, $x = (2.49 \pm 0.01)\ cm$. The two minima immediately encapsulating the global maximum occur at $x = (2.01 \pm 0.01)\ cm$ and $x = (2.98 \pm 0.01)\ cm$.

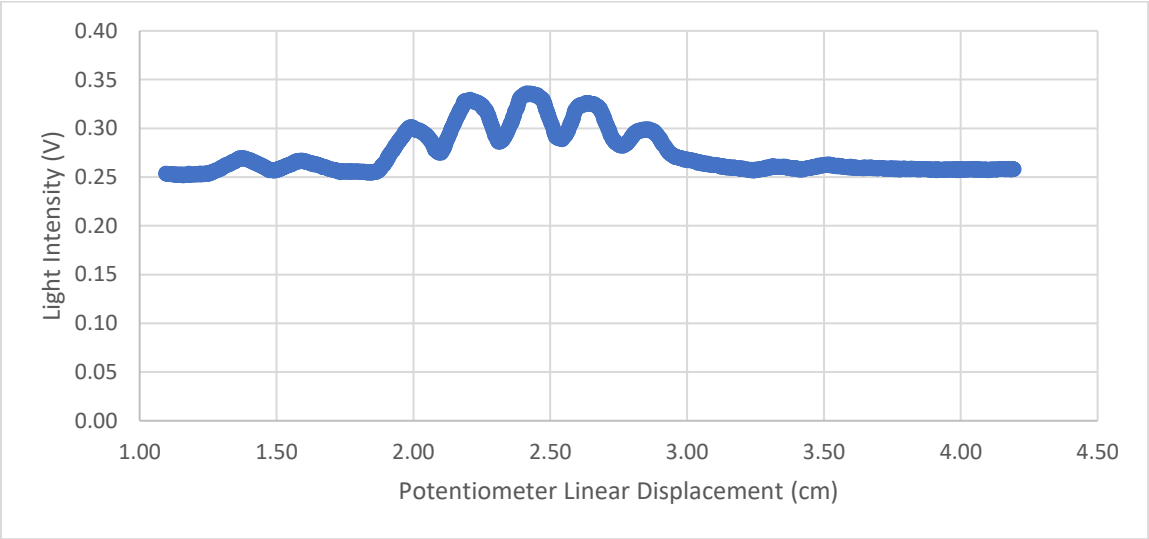

Figure 2: Diffraction Model Produced by a $0.00004\ m$-Wide Double Slit Diffraction Element with a Slit Distance of $0.0000125\ m$. As in Fig. (1), intensity data is measured by the photodiode and plotted against the sensor's linear displacement along the magnetic track. The global maximum occurs at $x = (2.42 \pm 0.01)\ cm$. Imagining a superposition of Fig. (1) onto this graph, Fig. (2)'s five centermost maxima would be contained within the peak of Fig. (1)'s global maximum. The minima immediately to the left and right of this peak are at $x = (1.91 \pm 0.01)\ cm$ and $x = (2.94 \pm 0.01)\ cm$.

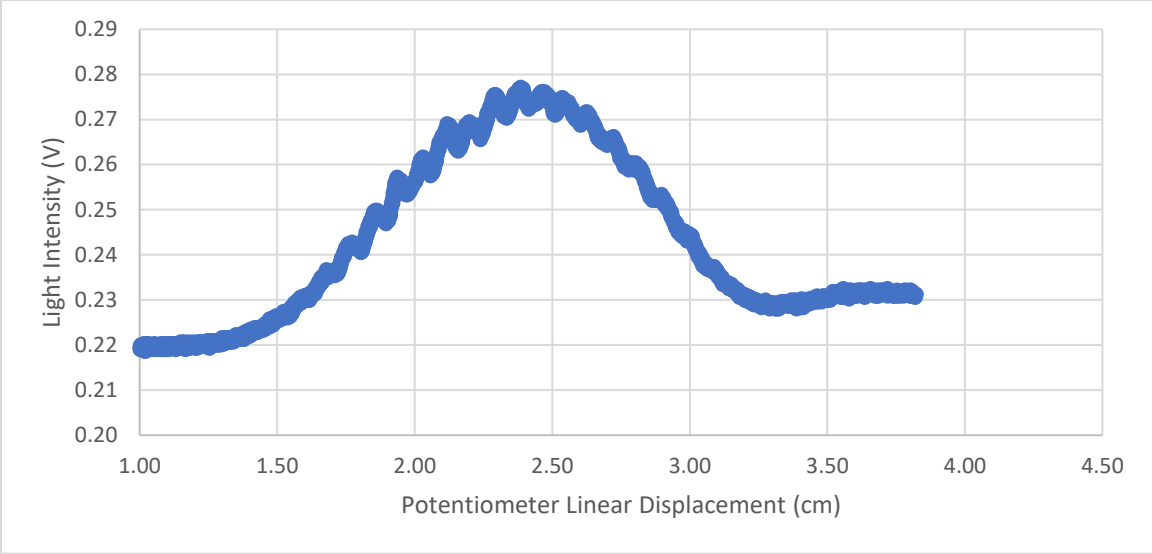

Figure 2: Diffraction Model Produced by a Double Slit Diffraction Element with Unknown Parameters. As in the previous two figures, intensity data is measured by the photodiode and plotted against the sensor's linear displacement along the magnetic track. The global maximum occurs at $x = (2.40 \pm 0.01)\ cm$. Again, the single slit diffraction model is an envelope function for this graph. The minima immediately to the left and right of the envelope's peak are at $x = (1.73 \pm 0.01)\ cm$ and $x = (3.09 \pm 0.01)\ cm$.

Next, we replace the photodiode in our experiment setup with a beam expander and diffraction grating with $600 \frac{lines}{mm}$. We position a protractor at the end of the grating to measure the angles of the diffracted beams, which represent maxima. We note that this configuration produces three distinct beams that are clearly visible by eye; however, the middle beam is slightly more defined than the outer two, which are at equal and opposite angles. Specifically, the three beams appear at angles of $(67.0 \pm 0.5)°$, $(90.0 \pm 0.5)°$, and $(113.0 \pm 0.5)°$. We replace the laser with a white light and remove the beam expander. Again, we observe three distinct beams clearly visible by eye. This time, the central beam is white, while the outer two have red, green, and blue ranges. The angular ranges for each color are displayed in Fig. (4).

Color	Angular Range (°)
Red	24.0 to 21.0
Green	21.0 to 19.0
Blue	19.0 to 17.0

Figure 4: Angular Ranges of Colors Produced by White Light Propagating through Diffraction Grating. Note that the colors are reflected at equal and opposite angles. The uncertainty associated with each angle is $\pm 0.5°$, as the protractor used for these measurements has whole number degree markings.

In our final procedure, we reintroduce the laser and aim it at a strand of human hair contained in a slide. A piece of paper stands $(0.4210 \pm 0.0005)\, m$ behind the slide to capture the diffracted beams. Recognizing that the resulting pattern behaves like that of a single slit diffracting element, we measure the distances between the center of the pattern and the minima. We find that the first-order minima occur at distances $(0.0350 \pm 0.0005)\, m$ and $(0.0370 \pm 0.0005)\, m$ from the center of the diffraction pattern. The second order minima occur at distances $(0.0720 \pm 0.0005)\, m$ and $(0.0730 \pm 0.0005)\, m$ from the center of the diffraction pattern.

3. Analysis

We use equation (2) to calculate an experimental value for the width of the single slit element. From our data in Fig. (1), we observe that the center of the diffraction pattern is at $(2.49 \pm 0.01)\, cm$. The first-order minima occur at $(2.01 \pm 0.01)\, cm$ and $(2.98 \pm 0.01)\, cm$. Thus, the distances of the minima from the center are $(0.48 \pm 0.01)\, cm$ and $(0.49 \pm 0.01)\, cm$. We evaluate equation (2) for b using these two distances as x values, as well as the given values $m = 1$, $\lambda = 6.7 * 10^{-7}$, and $D = (0.3190 \pm 0.0005)\, m$. We obtain $b = (0.000043 \pm 0.000003)\, m$ and $b = (0.000042 \pm 0.000003)\, m$, where the margins of uncertainty follow the formula:

$$\delta b = \sqrt{\left(\frac{m\lambda\delta D}{x}\right)^2 + \left(\frac{-m\lambda D\delta}{x^2}\right)^2}. \quad (6)$$

Averaging the calculated b values yields $b_{best} = (0.000042 \pm 0.000002)\, m$. The error is given by:

$$\delta b_{best} = \sqrt{\sum_{i=1}^{N} \left(\frac{\delta b_i}{N}\right)^2}. \tag{7}$$

Recalling that the actual width of the slit is $0.00004\, m$, we can determine the percent error associated with our experimental value with the formula:

$$\%\, error = \left|\frac{actual - experimental}{experimental}\right| * 100. \tag{8}$$

Hence, we find that the measured value has 5.0% error by equation (8). We also note that the actual value falls within the uncertainty of the experimental value; thus, b_{best} calculation corroborates equation (2).

Similarly, we use equation (4) to calculate experimental values for the slit distance in the double slit procedure. The relevant minima data comes from Fig. (2), and the values for λ and D are unchanged from the single slit calculation. We yield $d_{best} = (0.00001245 \pm 0.0000008)\, m$, where the margin of error is given by:

$$\delta d = \sqrt{\left(\frac{m\lambda\delta D}{x}\right)^2 + \left(\frac{-m\lambda D\delta}{x^2}\right)^2}. \tag{9}$$

Since the actual distance between the slits is $0.0000125\, m$, we use equation (8) to determine that our experimental value for d_{best} has 0.4% error. We also note that the actual value of d falls within the error boundary of d_{best}; thus, our data supports equation (4).

We hypothesize that the graph of Fig. (1) (single slit diffraction) is an envelope for the graph of Fig. (2) (known double slit diffraction). Thus, we may use the minima of the envelope function to determine the width of each double slit. From Fig. (2), we observe that the global maximum is at $(0.0242 \pm 0.0001)\, m$, while the first-order minima occur at $(0.0191 \pm 0.0001)\, m$ and $(0.0294 \pm 0.0001)\, m$. Thus, the distances from the minima to the center of the pattern are $(0.0051 \pm 0.0001)\, m$ and $(0.0052 \pm 0.0001)\, m$. From equations (2) and (6), we obtain the two values $b = (0.000041 \pm 0.000002)\, m$ and $b = (0.000040 \pm 0.000001)\, m$. The average is $b_{best} = (0.000040 \pm 0.000001)\, m$,

which is the actual value for the width of the slits. Thus, we confirm that the single slit diffraction pattern is an envelope for the double slit pattern.

Once more, we employ equations (4) and (9) to calculate experimental values for the slit distance and width for the known double slit procedure. The relevant minima data comes from Fig. (3), and the values for λ and D remain unchanged. We yield $d_{best} = (0.0000206 \pm 0.0000003)\, m$. As diffraction peaks become closer together, double slit spacing increases. Hence, we observe that peaks are closer together in Fig. (3) than they are in Fig. (2).

In Fig. (3), the global maximum is at $(0.0240 \pm 0.0001)\, m$, while the first-order minima occur at $(0.0309 \pm 0.0001)\, m$ and $(0.0173 \pm 0.0001)\, m$. The distances from the minima to the center of the pattern are $(0.0069 \pm 0.0001)\, m$ and $(0.0067 \pm 0.0001)\, m$. By equations (2) and (6), we obtain the two values $b = (0.000031 \pm 0.000002)\, m$ and $b = (0.000031 = 0 \pm 0.000001)\, m$. Thus, our calculated value for the width of each unknown double slit is $b_{best} = (0.000030 \pm 0.000001)\, m$.

From our examination of diffraction grating, we observe that increasing the number of slits reduces the total number of maxima while increasing each individual maximum's intensity. We measured that the laser produced a first-order maximum at an angle $(23.0 \pm 0.5)°$ from the middle beam. Converting to radians, we yield $\theta = (0.40 \pm 0.01)$. Because this is a first-order minimum, $n = 1$. Given $\lambda = 6.7 * 10^{-7}\, m$, we solve equation (5) to yield $d = (0.00000167 \pm 0.00000003)\, m$. The uncertainty in this result is given by:

$$\delta d = \frac{\delta\theta n\lambda \cos(\theta)}{\sin^2(\theta)}\,. \tag{10}$$

Since the actual distance is $\frac{1}{600000} m$, equation (8) gives us a percent error of 0.2%. We also observe that our experimental d contains the actual value within its error boundary, so our data agrees with equation (5).

From Fig. (4), we observe that the richest red light occurs at an angle of $(21.0 \pm 0.5)°$ from the middle beam. Converting to radians, we yield $\theta = (0.36 \pm 0.01)$. Likewise, the richest blue light occurs at an angle of $(17.0 \pm 0.5)°$ from the middle beam.

Converting to radians once again, we yield $\theta = (0.30 \pm 0.01)$. Using our experimental value for d and $n = 1$, we employ equation (5) to solve for the richest wavelengths of red and blue light. We yield $\lambda = (6.0 \pm 0.2) * 10^{-7}\, m$ and $\lambda = (4.9 \pm 0.2) * 10^{-7}\, m$, respectively. The error terms are given by:

$$\delta\lambda = \sqrt{\left(\delta d sin(\theta)\right)^2 + \left(d\delta cos(\theta)\right)^2}. \quad (11)$$

We can divide the speed of light, $c = 3.00 * 10^8 \frac{m}{s}$, by our experimental frequencies to yield the bandwidth for visible light. We calculate this range to be $(5.0 \pm 0.4) * 10^{14}\, Hz$ to $(6.1 \pm 0.4) * 10^{14}\, Hz$.

Finally, we use equation (2) with the minima data from our diffraction grating procedure to find the thickness of the human hair. Given $\lambda = (6.7 * 10^{-7})\, m$ and $D = (0.4210 \pm 0.0005)$, we calculate b for the x values $(0.0350 \pm 0.0005)\, m$, $(0.0370 \pm 0.0005)\, m$, $(0.0720 \pm 0.0005)\, m$, and $(0.0730 \pm 0.0005)\, m$. Using equation (6) to determine the uncertainty, we calculate that $b_{best} = (0.08 \pm 0.01)\, mm$. This is plausible, as further research confirms that human hair typically ranges in thickness from $0.04\, mm$ to $1.2\, mm$.

4. Conclusion

Our findings upheld equation (2), since the uncertainty term of our slit width calculation contained the actual width. Similarly, our calculated slit distance contained the actual distance within its error boundary; thus, our data agreed with equation (4). During this process, we also confirmed that the envelope for a double slit diffracting element is a single slit diffracting element of the same width. Moreover, our calculated value d in the laser diffraction grating procedure contained the expected value within its boundary; therefore, our data corroborated equation (5). Using our calculated d from equation (5), we revisited equation (2) to calculate the thickness of human hair, which fell within the normal range.

We also attempted to calculate the bandwidth for visible light using equation (5). We yielded the range $(5.0 \pm 0.4) * 10^{14}\, Hz$ to $(6.1 \pm 0.4) * 10^{14}\, Hz$. However, the actual

range is approximately $(4.0) * 10^{14}\ Hz$ to $(8.0) * 10^{14}\ Hz$. This inconsistency is likely a result of human error, as angle measurements were made by eye with a protractor. Because there were external sources of light in the laboratory room, some shades of diffracted light were difficult to see. To improve on this result in the future, it would be beneficial to conduct the experiment with a computerized method of measuring diffraction angles in a room without external light sources.